Journal Pre-proof

Sulfamethoxazole exposure to simulated solar radiation under continuous flow mode: Degradation and antibacterial activity

Carla Patrícia Silva, Cindy Oliveira, Ana Ribeiro, Nádia Osório, Marta Otero, Valdemar I. Esteves, Diana L.D. Lima

PII: S0045-6535(19)31837-5

DOI: https://doi.org/10.1016/j.chemosphere.2019.124613

Reference: CHEM 124613

To appear in: *ECSN*

Received Date: 15 May 2019

Revised Date: 1 August 2019

Accepted Date: 17 August 2019

Please cite this article as: Silva, Carla.Patrí., Oliveira, C., Ribeiro, A., Osório, Ná., Otero, M., Esteves, V.I., Lima, D.L.D., Sulfamethoxazole exposure to simulated solar radiation under continuous flow mode: Degradation and antibacterial activity, *Chemosphere* (2019), doi: https://doi.org/10.1016/j.chemosphere.2019.124613.

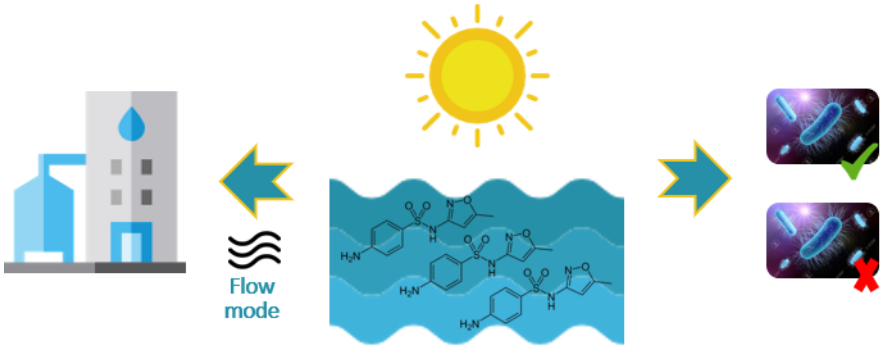

Sulfamethoxazole exposure to simulated solar radiation under continuous flow mode: degradation and antibacterial activity

Carla Patrícia Silva[a], Cindy Oliveira[b], Ana Ribeiro[c], Nádia Osório[c], Marta Otero[d], Valdemar I. Esteves[a], Diana L.D. Lima[a,e,*]

[a]CESAM & Department of Chemistry, University of Aveiro, Campus de Santiago, 3810-193 Aveiro, Portugal

[b]Department of Chemistry, University of Aveiro, Campus de Santiago, 3810-193 Aveiro, Portugal

[c]Instituto Politécnico de Coimbra, ESTESC-Coimbra Health School, Biomedical Laboratory Sciences Department, Rua 5 de Outubro, S. Martinho do Bispo, 3046-854 Coimbra, Portugal

[d]CESAM & Department of Environment and Planning, University of Aveiro, Campus de Santiago, 3810-193 Aveiro, Portugal

[e]Instituto Politécnico de Coimbra, ESTESC-Coimbra Health School, Complementary Sciences Department, Rua 5 de Outubro, S. Martinho do Bispo, 3046-854 Coimbra, Portugal

---

[*]*corresponding author*

Postal address: CESAM & Department of Chemistry, University of Aveiro, Campus de Santiago, 3810-193 Aveiro, Portugal

E-mail address: diana.lima@ua.pt

Abstract

Among pharmaceuticals, the occurrence of antibiotics in the environment is a subject of special concern due to their environmental impact, namely the development of bacterial resistance. Sulfamethoxazole (SMX) is one of the most commonly used antibiotics and it is regularly found, not only in effluents from sewage treatment plants (STPs), but also in the aquatic environment. Photodegradation appears as an alternative process for the removal of this type of pollutants from contaminated waters. In order to be used for a remediation purpose, its evaluation under continuous flow mode is essential, as well as the determination of the final effluent antibacterial activity, which were assessed in this work.

As compared with batch operation, the irradiation time needed for SMX elimination under continuous flow mode sharply decreased, which is very advantageous for the target application. Moreover, the interrelation between SMX removal, mineralization and antibacterial activity was evaluated before and during photodegradation in ultrapure water. Although mineralization was slower than SMX removal, bacterial activity increased after SMX photodegradation. Such an increase was also verified in environmental water matrices. Thus, this study has proven that photodegradation is an efficient and sustainable process for both (i) the remediation of waters contaminated with antibiotics, and (ii) the minimization of the bacterial resistance.

Keywords: Photolysis; Sulfonamides; Continuous flow water treatment; Antibacterial activity; Vibrio fischeri

1. Introduction

Water quality constitutes an issue widely discussed since it is essential to human wellbeing, health and activities, as well as to the preservation of aquatic life. Emerging contaminants, as antibiotics, end up in aquatic resources at concentrations that, even though very low, are known to induce undesirable effects on ecosystems (Meffe and Bustamante, 2014) and negative impact on water quality. The main cause of the presence of these contaminants in the aquatic environment is the inefficiency of conventional treatments applied in sewage treatment plants (STPs).

In the European context, there are no regulated discharge limits for pharmaceuticals, still some directives have been published. The first mark in the European water policy was the Directive 2000/60/EC, which focused on prioritizing substances presenting a high risk. This was amended by the Directive 2008/105/EC, which settled a group of 33 priority substances or groups of substances. More recently, Directive 2013/39/EU enlarged this group to 45 priority substances or groups of substances, recommending attention to either monitoring and treatment options. Then, the Decision 2015/495/EU set the first watch-list of substances for European Union wide-monitoring, which included three antibiotics amongst 17 organic compounds (Barbosa et al., 2016). Implementing Decision (EU) 2015/495 was next repealed by Decision 2018/840/EU, which set a new watch-list that added two more antibiotics to those already included in the first list. This evolution shows the concern to cover an ever-increasing group of compounds as well as to improve and/or develop new treatments and/or strategies for their removal from water.

Water treatment processes usually mimic or build on natural processes, either biological, chemical or physical, that have been observed to favour the removal of contaminants from water. In the case of antibiotics, they may undergo different processes in the aquatic environment that affect their fate and represent the reduction of their concentration, like biodegradation, sorption, hydrolysis or photodegradation (Charuaud et al., 2019).

Photodegradation appears to be the major antibiotics' degradation pathway in surface waters (Charuaud et al. 2019). Two types of photodegradation may occur in natural waters: direct photolysis (the target antibiotic absorbs photons able to induce chemical transformations (Oliveira et al., 2019)) and indirect photolysis (other substances, which are called photosensitizers, absorb solar radiation, transferring energy to the pollutant or generating reactive oxygen species (ROS; hydroxyl radicals, $OH^{\bullet}$; peroxyl radicals, $ROO^{\bullet}$; singlet oxygen, $^{1}O_2$) (Carlos et al., 2012) that induce the photodegradation). In any case, photolysis means the degradation of antibiotics and, therefore, may account for their removal (Lin et al., 2019; Norvill et al., 2017). Moreover, solar radiation being plentiful and free, utilization of natural light for the removal of antibiotics is a green, sustainable and environmentally-friendly approach.

Regarding the industrial application of photodegradation, it is important that the process runs continuously (Suhadolnik et al., 2019). Therefore, the assessment of antibiotics' photodegradation in continuous flow mode is essential for application as tertiary advanced treatment in STPs. In this sense, Pretto et al. (2018) and Zhong et al. (2018) assessed the photocatalysis of the antibiotics sulfamethoxazole (SMX) and tetracycline (TC), respectively, in flow mode. Recently, and to avoid photocatalysts

assistance, Lin et al. (2019) designed a novel system that combined sunlight-focusing coupled with a solar tracking (SFST). These authors successfully used the SFST system for the photodegradation of SMX and ciprofloxacin in a quartz reactor tank under continuous operation. However, to the best of the authors' knowledge, there are no research works dealing with the solar simulated photodegradation of antibiotics in tubular reactors operated under continuous flow mode and in absence of synthetic materials acting as photocatalysts. This fact constitutes, therefore, the main novelty of this work, in which the photodegradation of SMX under simulated solar radiation was investigated in a tubular reactor operated in continuous flow mode. In addition, after observing that SMX photodegradation was affected by matrix effects under batch operation (Oliveira et al., 2019), continuous flow mode using different water matrices (ultrapure, fresh, estuarine and STP effluent) was assessed in this work. Another aim of this study was to gain insight on the bacterial resistance problem either in what respects the parent compound and possible photodegradation products. For that purpose, antibacterial activity of the initial and photodegraded SMX solutions using the *Vibrio fischeri* microorganism was evaluated in the different water matrices tested. Finally, the relation between SMX photodegradation, its mineralization and antibacterial activity was assessed.

2. Materials and methods

2.1. Reagents and standards

SMX (> 98%) was provided by TCI (Europe). Acetonitrile (HPLC grade) and acetic acid (p.a.) used for high-performance liquid chromatography with a fluorescence

detector (HPLC-FD) analysis, were obtained from VWR and Prolabo, respectively. Ultrapure water, used in the preparation of solutions, was obtained from a Millipore system (Milli-Q plus 185). Nutrient Broth nº2 supplemented with 2% of NaCl (Oxoid, UK) was used to grow the bacteria in the antibacterial activity tests.

2.2. Water matrices

Surface waters (fresh and estuarine) and effluent from a STP were collected in ambar glass bottles. The latter was collected in a STP designed to serve 159 700 population equivalents, receiving an average daily flow of 39 278 m^3 day^{-1}. In this STP, sewage is subjected to primary and biological treatment and the collection was performed after the biological decanter, which corresponds to the final treated effluent that is discharged in the environment, which for this specific STP occurs at ~3 km from the coast, on the Atlantic Ocean. This matrix will be referred onwards as STPF. After collection, all water matrices were filtered through 0.22 μm nitrocellulose membrane filters (Millipore) avoiding bacteria activity and stored at 4 ˚C prior to use. All the water matrices were characterized through UV-visible spectrophotometry, atomic absorption spectrophotometry and measuring different parameters, such as dissolved organic carbon (DOC), salinity, pH and conductivity. The employed methods are detailed elsewhere (Oliveira et al., 2019) and the corresponding results are shown in Table S1 as supplementary data.

2.3. Chromatographic analysis

Quantitative analysis of SMX was achieved using HPLC-FD. The device consisted of a degasser DGU-20A5R, a column oven CTO-10AC, a pump LC-30AD and an autosampler SIL-30AC (all from Shimadzu). For the separation, a Kinetex XB-C18 column (2.6 μm, 100 mm x 4.60 mm) was used. Both the cell and column temperature were maintained at 25 °C and an injection of 20 μL was used. The mobile phase consisted of water (acidified with 1% acetic acid):acetonitrile mixture (40:60, *v/v*) and the flow rate was maintained at 0.8 mL min^{-1}. Before use, acidified water and acetonitrile were filtered through a 0.2 μm polyamide membrane filters (Whatman). The detection of SMX was done by using a Prominence RF-20Axs fluorescence detector from Shimadzu with an excitation wavelength of 265 nm and an emission wavelength of 343 nm.

The SMX calibration curve was obtained by preparation of standard solutions in ultrapure water, with concentrations 100, 50, 25, 10, 5 and 1 μg L^{-1}, by dilution of proper amounts of the stock solution.

2.4. Photodegradation experiments

2.4.1. Apparatus and experimental procedure description

All SMX solutions were irradiated under simulated solar radiation using a Solarbox 1500 (Co.fo.me.gra, Italy). The irradiation device contained an arc xenon lamp (1500 W) and outdoor UV filters that limited the transmission of light with wavelengths below 290 nm. The irradiance of the lamp was set to 55 W m^{-2} (290-400 nm) and was kept constant during all the experiments. To monitor the irradiance level and temperature, a multimeter (Co.fo.me.gra, Italy), equipped with a UV (290-400 nm)

large band sensor and a black standard temperature sensor, was used. Through an air-cooled system, the device was refrigerated. Furthermore, a parabolic reflection system guaranteed the uniformity of the irradiation inside the chamber.

The apparatus used to study the SMX photodegradation in continuous flow mode is represented in Fig. 1. In this apparatus, irradiation and control experiments were carried out simultaneously. For this purpose, 20 mL reservoirs containing SMX solutions (one for the solution to be irradiated and another for the control) were capped with Parafilm M® and covered with aluminum foil to protect the solution from light. Both solutions were pumped with a Longer Pump BT 100-1L, using a flow rate of 150.1 $\mu L\ min^{-1}$, through respective narrow-bore (inner diameter: 0.8 mm and outer diameter: 1.6 mm) transparent tubes of fluorinated ethylene propylene from Adtech Polymer Engineering Ltd (UK). Each of the two tubes had a total length of 2.80 m, however, just 1.50 m were inside the Solarbox, while the rest, which was outside to allow for recirculation, was covered with aluminium foil to protect the solution from light. As shown in Fig. 1, tubing inside the Solarbox was bent into 10 loops and arranged horizontally over a flat plate (18.5 x 27 cm) in order to maximize the exposed surface area. On the other hand, from the two plates inside the Solarbox, the one corresponding to the control was covered with aluminum foil to protect the SMX solution from light while subjected to identical conditions and during the same time as the irradiated solution. During the experiments, SMX solutions circulated continuously through the described apparatus, aliquots being periodically withdrawn in order to determine the concentration of SMX along time. The simultaneous non-irradiated controls were used to verify that the SMX concentration remained stable during the experiments and to have a reference for the calculation of the percentage of degradation under irradiation.

This way, the decrease of SMX concentration in exposed solutions can be ascribed solely to photo-induced degradation.

Figure 1

2.4.2. SMX photodegradation

A SMX stock solution of 100 mg L^{-1} was prepared by dissolving SMX in ultrapure water and then kept at 4 °C in the dark.

SMX photodegradation in ultrapure water and in different water matrices (fresh, estuarine and STPF) was studied under the experimental procedure described in the previous section. SMX solutions of 100 μg L^{-1} were prepared in ultrapure water by dilution of the stock solution for the studies on direct photodegradation, which had a maximum duration of 1 h. For the study of matrix effects, SMX solutions in the different filtered water matrices were prepared by spiking each of them with 100 μg L^{-1} of SMX. Irradiation experiments for the study of matrix effects had a maximum duration of 5 h.

2.5. Antibacterial activity and SMX mineralization

For the evaluation of the SMX mineralization along photodegradation and the antibacterial activity of SMX photoproducts, the direct photodegradation of a 100 mg L^{-1} SMX solution was performed following the procedure above described. The relatively high concentration used was needed to detect variations in the bacterial growth in the presence of the SMX solution and to follow the organic carbon content during the irradiation process.

The SMX mineralization and the antibacterial activity were determined at the beginning of the SMX photodegradation experiments (t_0, 0 h), after 50% of SMX photodegradation (t_1, 0.74 h), after 95% of SMX photodegradation (t_2, 14 h) and when no SMX was detected by HPLC-FLD (t_3, 49 h). A non-irradiated blank of ultrapure water with no SMX was used as control (sample A). Also, a SMX standards with 50% and 100% of the initial concentration (100 mg L^{-1}) but not subjected to any irradiation were used for comparison with irradiated sample (therefore containing any photoproducts formed during the irradiation).

In order to assess SMX mineralization, DOC was measured in samples from the direct photodegradation experiments using a Total Organic Carbon analyser, TOC-V_{CPH}, from Shimadzu. Samples were acidified with 2% (*v/v*) of HCl 2 mol L^{-1}, purged with nitrogen and covered with Parafilm M®, previously to the analysis.

Tests of antibacterial activity were performed using *Vibrio fischeri* ATCC 7744 incubated overnight in Nutrient Broth n.2 supplemented with 2% of NaCl. The strain was grown to optical density (OD) 0.9 at wavelength 600 nm and then was used in the bioassays in ultrapure water and in the different environmental water samples. All assays were performed in triplicate. The cytotoxic effect was evaluated considering the bacterial growth at a wavelength of 600 nm and its bioluminescence at a wavelength of 420 nm using a Multiskan™ GO, Thermo Scientific, UK.

Antibacterial tests were also performed for the indirect photodegradation of a 100 mg L^{-1} SMX in the different water matrices (fresh, ultrapure and STPF) at the corresponding t_0, t_1, t_2 and t_3. As for the direct photodegradation experiments, a non-irradiated blank of the water matrix with no SMX was used as control (sample A) and

non-irradiated SMX standards with 50% and 100% of the initial concentration (100 mg L^{-1}) in the corresponding matrix were used for comparison purposes.

In all the matrices (ultrapure, fresh, estuarine and STPF water), the percentage of viable cells was estimated at wavelength 420 nm using Eq. 1:

$$\%\ of\ viable\ cells = \left(\frac{OD\ in\ test}{OD\ in\ sample\ A}\right) \times 100 \qquad \text{Eq. 1}$$

3. Results and Discussion

3.1. Photodegradation kinetics of SMX in ultrapure water and environmental water matrices

Photodegradation of SMX in ultrapure water and environmental water matrices was monitored by the determination of the antibiotic concentration in the aliquots, experiments enduring until no SMX was detected in the irradiated solutions. Experimental results were fitted by non-linear regression to the pseudo first-order kinetic model, according to Eq. 2:

$$C/C_0 = e^{-kt} \qquad \text{Eq. 2}$$

where, C is the SMX concentration in the solution exposed to light at different irradiation times (µg L^{-1}); C_0 is the SMX concentration in the solution protected from light at different irradiation times (µg L^{-1}); k is the pseudo first-order degradation rate constant (h^{-1}); and t is time (h).

Kinetic curves of SMX photodegradation in ultrapure water and in different environmental water matrices are presented in Fig. 2. The obtained data for the variation of SMX concentration along irradiation time were fitted to a pseudo first-order kinetic

model. Moreover, the corresponding parameters (photodegradation rate (k (h^{-1})) and half-life time ($t_{1/2}$ (h), (calculated as ln2/k)) are presented in Table 1. No degradation was observed in the non-irradiated control solutions, indicating that, under the experimental conditions employed, and in the matrices used, SMX degradation by other means than irradiation (such as microbiological or thermal means) is negligible.

Figure 2

Overall, and as it can be seen either in Fig. 2 and Table 1, SMX underwent very fast photodegradation in ultrapure water ($t_{1/2}$ = 0.32 h). However, when present in environmental samples, the SMX photodegradation rate markedly decreased with the respective increase in $t_{1/2}$ ($t_{1/2}$ between 0.95 and 1.5 h). SMX photodegradation rate increased in the order: STPF ≈ estuarine water < freshwater < ultrapure water. In the latter, after 45 min of irradiation, a photodegradation of 81.4% was observed, while for the fresh, estuarine, and STPF water matrices, photodegradation was 47.5%, 42.8%, and 37.6%, respectively. As stated in Oliveira et al. (2019), DOC analysis indicated that the STPF matrix had the greatest content of organic carbon (26.45 mg L^{-1}). That may account for the complexity of the sample and for a higher inner filter effect in this matrix, which reduces the available radiation for SMX photodegradation, eliciting the lower photodegradation rate.

Table 1

The STPF matrix was the one showing the lowest efficiency to induce the SMX photodegradation, which resulted in a $t_{1/2}$ 4.7 times higher than that observed in ultrapure water (1.5 ± 0.1 h and 0.32 ± 0.03 h, respectively).

Overall, it is possible to conclude that the environmental water matrices cause a great delay in the photodegradation of the SMX. To better understand the SMX photodegradation under environmental conditions, $t_{1/2}$ (h) may be converted to summer sunny days (SSD). These $t_{1/2}$ (SSD) were calculated using the assumption that 1 SSD (24 h) will correspond to 3.8 h of irradiation (knowing that the total energy reaching the ground on a SSD, for 45 ºN latitude is 7.5×10^5 J m^{-2}) (Silva et al., 2016). As depicted in Figure 3, 0.085 ± 0.007 SSD were needed to reach $t_{1/2}$ in ultrapure water, while in environmental matrices the SSD varied between 0.27 ± 0.02 and 0.39 ± 0.03.

Figure 3

In what regards the comparison between SMX photodegradation under batch (Oliveira et al., 2019) and continuous flow mode (this work), Table 1 and Figure 3 represent the determined parameters corresponding to each operation mode. As shown in Table 1, the increase in k (h^{-1}) and the respective decrease in $t_{1/2}$ (h) under continuous flow mode as compared with batch is clear. Still, differences depended on the matrix, so, for example, in ultrapure water, the $t_{1/2}$ (h) is 2.7 times smaller under continuous flow than under batch conditions, while in freshwater it is 5.8 times smaller than under batch mode (Oliveira et al. 2019). Fig. 3, which represents $t_{1/2}$ (SSD), highlights the differences between batch and continuous flow modes. For example, for the case of the estuarine sample, $t_{1/2}$ (SSD) was reduced from 1.4 (batch mode) to 0.37 (flow mode). It is therefore noticeable that SMX photodegradation under continuous flow mode is more efficient than under batch conditions, especially in environmental water matrices. This must be related to the enhanced light penetration and distribution inside the solution, which are the dominant factors in the design of efficient photo-reactors. The reduced optical thickness (0.4 mm) and narrowness (0.8 mm internal diameter) of tubing favours

light penetration while circulation in continuous flow mode facilitates light intensity distribution and homogeneous conditions in the SMX solution that is inside. On the other hand, the arrangement of the tubing in a loop pattern increases the ratio of irradiated volume and residence time to the irradiated surface area so improving the effectiveness of light exposition.

Higher degradation rates, resulting in lower $t_{1/2}$, for the flow mode in comparison with the batch mode had already been observed by Fernández et al. (2017) for the photocatalysts-assisted E2 degradation in a channelled reactor. However, to the best of the authors' knowledge, this is the first assessment of the potential application of photodegradation under continuous flow mode for the removal of antibiotics as an effluent treatment option. Results obtained are promising for the development of an economically viable green water treatment technology aiming at the photodegradation of antibiotics under solar radiation, continuous flow systems being simply integrated as tertiary treatments in existing STPs. On the other hand, a relevant feature of the here used design lies in the loop arrangement of tubing, which increases the solution residence time and operating volume of the reactor, while occupying a reduced physical area. Similar patterns have been reported for algal tubular photobioreactors used for water treatment (Lv et al., 2017; Villaseñor-Camacho et al., 2018), in which photolysis might be also involved in the removal of pollutants (Vo et al., 2019).

3.2. Antibacterial activity and SMX mineralization

Vibrio fischeri ATCC 7744 was chosen to represent bacteria present in environmental waters because it is known to play an important role in antibiotics'

resistance dissemination (Backhaus and Grimme, 1999; Cabral, 2010; Chavez-dozal et al., 2013). Also, *Vibrio fischeri* detection is relatively simple since metabolically active cells emit bioluminescence. Therefore, the bacterial growth was correlated with its bioluminescence. The representation of OD at 400 nm (bioluminescence) versus OD at 600 nm (bacterial growth) showed that the higher the bioluminescence, the greater the bacterial growth. This positive correlation supports the utilization of bioluminescence data for the interpretation of the cytotoxic effect of the samples under study. Then results obtained from the antibacterial activity tests are shown in (Fig. 4 a-d).

Figure 4

From the analysis of Fig. 4a, a higher bacterial growth can be observed in sample A since no antibiotic was present, only ultrapure water. Thus, this bacterial growth corresponds to that of the culture medium where the *Vibrio fischeri* bacteria was grown. On the other hand, in sample D there was the greatest inhibition of bacterial growth, which corresponds to antimicrobial activity of the non-irradiated control, containing the highest SMX concentration tested (100 mg L^{-1}). All samples B, C and E have the same SMX concentration (50 mg L^{-1}) and similar antibacterial activity. Also, similar results obtained for sample C and E, which was subjected to irradiation, indicate that photodegradation products that might be produced until $t_{1/2}$, do not influence the bacterial growth. As for samples F and G, similar bacterial activity was observed, which was higher than the presented by sample D, being these results statistically different (ρ value = 0.01).

Results on TOC removal are shown in Fig. 5 together with SMX photodegradation and *Vibrio fischeri* viable cells. As may be seen, when 95% of SMX

was removed by photodegradation, only 10% of mineralization occurred (sample F). However, the % of *Vibrio fischeri* viable cells significantly increased when compared with the control sample (sample D). In sample G, when no SMX was detected and bacterial activity was equivalent to F, only around 35% of mineralization was observed. Therefore, direct photolysis provided for the complete photodegradation of SMX to intermediate photoproducts, but not for the mineralization of the latter. The low mineralization of SMX by direct photolysis has already been reported by other authors (Gong and Chu, 2016; Mouamfon et al., 2010; Wu et al., 2019). Notwithstanding, in this work, from the results obtained in ultrapure water, it can be concluded that the SMX photodegradation, even when not associated to equivalent mineralization, leads to a loss of the solution antibacterial activity and, in the case of formation of photoproducts, these not exhibit higher antibacterial activity than SMX. This indicates that the photodegradation treatment results in the minimization of bacterial resistance. With regards to SMX mineralization (Fig. S1 in supplementary data), almost 70% of TOC reduction was observed after 83 h.

Regarding indirect SMX photodegradation in freshwater, Fig. 4b evidences that sample A did not exhibit the highest bacterial growth (bacterial growth in freshwater matrix was lower than the obtained in the culture medium) even though SMX was absent. This indicates that the matrix solution has an influence on the bacterial growth. As previously observed in ultrapure water, sample D was the one showing the largest inhibition of bacterial growth, indicating the antimicrobial activity of SMX. Although SMX concentration and irradiation times were different, samples A, B, C and D did not statistically differ, which again points out that the matrix had a great effect on bacterial growth. Sample D and E were statistically different (ρ value = 0.01), with a higher

bacterial activity observed for sample E, indicating that photodegradation reduced the antibacterial activity of SMX. Sample E and F were also statistically different (ρ value = 0.01), sample F presenting higher activity. This suggests that photoproducts may have higher antibacterial activity than SMX or that the matrix compounds' photodegradation may result in harmful compounds with antibacterial activity (which would need more irradiation time to photodegrade than SMX). However, in sample G the bacterial activity increased with respect to sample F (statistically different for ρ value = 0.001), indicating that possible photoproducts formed in sample F disappeared with the increase of irradiation time. Once again it was proven that, for this particular case study, photodegradation was efficient in the elimination of compounds that might increase the bacterial resistance if the time used is sufficient.

Results of antibacterial activity obtained in estuarine water are presented in Fig. 4c. As observed in freshwater, sample A did not exhibit the highest bacterial growth, indicating once again that the compounds present in the estuarine water matrix have the ability to inhibit the bacterial growth. As observed in Fig. 4a and 4b, the higher inhibition of bacterial growth was observed in sample D, which indicates the SMX antimicrobial activity. Samples A to E were not statistically different, although SMX concentration and irradiation times were different. However, sample D and F were statistically different (for ρ value = 0.05), with higher bacterial activity in sample F, indicating that photodegradation reduced the SMX antibacterial activity.

Finally, antibacterial tests were performed in STPF matrix (Fig. 4d). Samples were not statistically different, which did not allow to reach important conclusions about the SMX antibacterial activity in this matrix. Probably, effects on bacterial

390 growth by the STPF matrix and compounds present in it are masking those by SMX,
391 even when the spiked concentration was relatively high. This observation may be due to
392 the fact that the STPF matrix may have in its constitution other compounds (namely
393 other antibiotics) harmful to the *Vibrio fischeri* bacteria. Osorio et al. (2016) concluded
394 that synergistic effects may largely enhance the overall effects of individual components
395 in complex matrices, such as wastewater overall toxicity of complex.

396 In literature, few studies dealt with the resistance of *Vibrio fischeri* towards SMX,
397 using photodegradation under simulated sunlight irradiation (Gmurek et al., 2015; Niu
398 et al., 2013; Trovó et al., 2009). These authors found that inhibition of *Vibrio fischeri*
399 luminiscence by SMX photodegradation products was equivalent to that by the parent
400 antibiotic (Gmurek et al., 2015; Niu et al., 2015) or slightly higher but not reaching toxic
401 levels (Trovó et al., 2009). However, these works were carried out for the products from
402 the direct photolysis of SMX (in ultrapure or distilled water). Therefore, the studies
403 performed in this work represent a step forward in the knowledge about the antibacterial
404 resistance related to SMX and its photodegradation in environmental water matrices.

405

406 **Conclusions**

407 Occurrence of the antibiotic SMX in aquatic environments is widely discussed in
408 literature and, being STPs a main source, its removal from effluents before discharge is
409 imperative, mainly to prevent the spread of bacterial resistance. Photodegradation can
410 be applied as a remediation process, e.g. as a tertiary treatment in a STPs. With this in
411 mind, SMX photodegradation was here studied under continuous flow mode, irradiation
412 being done over circulating solutions through transparent tubing horizontally arranged

in a loop pattern. Photodegradation of SMX in ultrapure water and environmental water matrices (fresh, estuarine and STPF) was assessed. Furthermore, photodegradation of SMX under continuous flow was compared with batch mode, proving that the first was much faster as for the enhanced light penetration and distribution. Compared with ultrapure water, a larger efficiency occurred in the environmental water matrices, with $t_{1/2}$ (h) being 3.8-5.8 times shorter under continuous than batch mode. Along with SMX photodegradation experiments in ultrapure water, TOC concentration and viability of *Vibrio fischeri* cells were evaluated, showing that SMX mineralization was slower than photodegradation but resulted in the increase of bacterial activity. The increase of bacterial activity with SMX photodegradation was also verified in fresh and estuarine water. However, in the STPF sample, background inhibition masked photodegradation effects of SMX photodegradation on bacterial activity of *Vibrio fischeri*. From all the above, photodegradation under continuous flow mode may be considered a promising, sustainable and alternative option for application in the removal of antibiotics from contaminated effluents (e.g. from STPs, aquaculture enterprises, pharmaceutical companies, hospitals, etc.).

Acknowledgements

This work was funded by FEDER through CENTRO 2020 and by national funds through FCT within the research project PTDC/ASP-PES/29021/2017. Marta Otero thanks support by FCT Investigator Program (IF/00314/2015). Diana Lima was funded by national funds (OE), through FCT Fundação para a Ciência e a Tecnologia, I.P., in the scope of the framework contract foreseen in the numbers 4, 5 and 6 of the article 23,

of the Decree-Law 57/2016, of August 29, changed by Law 57/2017, of July 19. Thanks are due, for the financial support to CESAM (UID/AMB/50017/2019), to FCT/MCTES through national funds. STP workers are acknowledged for the kind assistance at wastewater collection.

References

Backhaus, T.; Grimme, L.H.; The toxicity of antibiotic agents to the luminescent bacterium *Vibrio fischeri*; Chemosphere 38 (1999) 3291.

Barbosa, M.O.; Moreira, N.F.F.; Ribeiro, A.R. Pereira, M.F.R.; Silva, A.M.T.; Occurrence and removal of organic micropollutants: An overview of the watch list of EU Decision 2015/495; Water Research 94 (2016) 257.

Cabral, P.S.J.; Water Microbiology. Bacterial Pathogens and Water; International Journal of Environmental Research and Public Health 7 (2010) 3657.

Carlos, L.; Mártire, D.O.; Gonzalez, M.C.; Gomis, J.; Bernabeu, A.; Amat, A.M.; Arques, A.; Photochemical fate of a mixture of emerging pollutants in the presence of humic substances; Water Research 46 (2012) 4732.

Chavez-dozal, A.; Gorman, C.; Erken, M.; Steinberg, P.D.; Mcdougald, D.; Nishiguchi, K.; Predation Response of Vibrio fischeri Biofilms to Bacterivorus Protists; Journal Applied and Environmental Microbiology 79 (2013) 553.

Charuaud, L.; Jarde, E.; Jaffrezic, A.; Thomas, M.-F.; Le Bot, B; Veterinary pharmaceutical residues from natural water to tap water: Sales, occurrence and fate; Journal of Hazardous Materials 361 (2019) 169-186.

458 Fernández, L.; Borzecka, W.; Lin, Z.; Schneider, R.J.; Huvaere, K.; Esteves, V.I.; Cunha,
459 Â; Tomé, J.P.C.; Nanomagnet-photosensitizer hybrid materials for the degradation of 17β-
460 estradiol in batch and flow modes; Dyes and Pigments 142 (2017) 535.

461 Gmurek, M.; Horn, H.; Majewsky, M; Phototransformation of sulfamethoxazole under
462 simulated sunlight: Transformation products and their antibacterial activity toward *Vibrio*
463 *fischeri*; Science of the Total Environment 538 (2015) 58.

464 Gong, H.; Chu, W.; Determination and toxicity evaluation of the generated products in
465 sulfamethoxazole degradation by UV/CoFe2O4 /TiO2. Journal of Hazardous Materials 314
466 (2016) 197.

467 Lin, Y.-C.; Panchangam, S.C.; Liu, L.-C.; Lin, A.Y.-C.; The design of a sunlight-
468 focusing and solar tracking system: A potential application for the degradation of pharmaceuticals
469 in water; Chemosphere 214 (2019) 452-461.

470 Lv, J.; Feng, J.; Liu, Q.; Xie, S.; Microalgal cultivation in secondary effluent: Recent
471 developments and future work. International Journal of Molecular Sciences 18 (2018) 79.

472 Meffe, R.; Bustamante, I.; Emerging organic contaminants in surface water and
473 groundwater: A first overview of the situation in Italy; Science of the Total Environment 481
474 (2014) 280.

475 Mouamfon, M.V.N.; Li, W.; Lu, S.; Qiu, Z.; Chen, N.; Lin, K.; Photodegradation of
476 sulphamethoxazole under UV-light irradiation at 254 nm. Environmental Technology 31 (2010),
477 489.

478 Niu; J.; Zhang, L.; Li, Y.; Zhao, J.; Lv, S.; Xiao, K.; Effects of environmental factors on
479 sulfamethoxazole photodegradation under simulated sunlight irradiation: Kinetics and
480 mechanism; Journal of Environmental Sciences 25 (2013) 1098.

Norvill, Z.N., Toledo-Cervantes, A., Blanco, S., Shilton, A., Guieysse, B., Muñoz, R.; Photodegradation and sorption govern tetracycline removal during wastewater treatment in algal ponds; Bioresource Technology 232 (2017) 35-43.

Oliveira, C.; Lima, D.L.D.; Silva, C.P.; Calisto, V.; Otero, M.; Esteves, V.I.; Photodegradation of sulfamethoxazole in environmental samples: The role of pH, organic matter and salinity; Science of the Total Environment 648 (2019) 1403.

Osorio, V.; Sanchís, J.; Abad, J.L.; Ginebreda, A.; Farré, M.; Pérez, S.; Barceló, D.; Investigating the formation and toxicity of nitrogen transformation products of diclofenac and sulfamethoxazole in wastewater treatment plants; Journal of Hazardous Materials 309 (2016) 157.

Pretto, P.R.P.; Palácio, S.M.; Campos, E.A., Pazini, C.R.; Veit, M.T.; Sulfamethoxazole photocatalytic degradation in a continuous flow reactor using artificial radiation; Journal of Environmental Chemical Engineering 6 (2018) 1926.

Silva, C.P.; Lima, D.L.D.; Groth, M.B.; Otero, M.; Esteves, V.I.; Effect of natural aquatic humic substances on the photodegradation of estrone; Chemosphere 145 (2016) 249.

Suhadolnik, L.; Pohar, A.; Novak, U.; Likozar, B.; Mihelič, A.; Čeh, M.; Continuous photocatalytic, electrocatalytic and photo-electrocatalytic degradation of a reactive textile dye for wastewater-treatment processes: Batch, microreactor and scaled-up operation; Journal of Industrial and Engineering Chemistry 72 (2019) 178-188.

Trovó, A.G.; Nogueira, R.F.P.; Agüera, A.; Sirtori, C.; Fernández-Alba, A.R.; Photodegradation of sulfamethoxazole in various aqueous media: Persistence, toxicity and photoproducts assessment; Chemosphere 77 (2009) 1292.

Villaseñor-Camacho, J.; Fernández Marchante, C.M.; Rodríguez Romero, L.; Analysis of a photobioreactor scaling up for tertiary wastewater treatment: denitrification, phosphorus removal, and microalgae production. Environmental Science and Pollution Research 25 (2018) 29279-29286.

506 Vo, H.N.P.; Ngo, H.H.; Guo, W.; Nguyen, T.M.H.; Liu, Y.; Nguyen, D.D.; Chang, S.W.;
507 A critical review on designs and applications of microalgae-based photobioreactors for pollutants
508 treatment; Science of the Total Environment 651 (2019) 1549-1568.

509 Wu, C.H.; Kuo, C.Y.; Dong, C.D.; Chen, C.W.; Lin, Y.L.; Removal of sulfonamides
510 from wastewater in the UV/TiO2 system: Effects of pH and salinity on photodegradation and
511 mineralization. Water Science and Technology 79 (2019) 349.

512 Zhong, S.; Lv, C.; Zou, S.; Zhang, F.; Zhang, S.; Preparation of pumice-loaded
513 CeO2/Bi2WO6 photocatalysts and treatment of tetracycline wastewater with a continuous flow
514 photocatalytic reactor; Journal of Materials Science: Materials in Electronics 29 (2018) 2447-
515 2454.

516

Fig. 1: Scheme of the apparatus used in this work to study SMX photodegradation in continuous flow mode.

Fig. 2: Kinetics of SMX photodegradation under continuous flow mode when present in ultrapure water (×) and in environmental matrices (Estuarine water (●); Freshwater (◊); STPF (□)). Experimental results are represented together with fittings to the pseudo first-order kinetic model.

Fig. 3: Comparison between $t_{1/2}$ (SSD) obtained in the different water matrices under batch mode (Oliveira et al., 2019) and continuous flow mode (this work), respectively represented in white and grey.

Fig. 4: Percentage of *Vibrio fischeri* viable cells in a) A - Ultrapure water (matrix) without SMX and without irradiation; B - control without irradiation (50 mg L^{-1} SMX); C - control covered with aluminum at t_3 of irradiation (50 mg L^{-1} SMX); D - control covered with aluminum at t_3 of irradiation (100 mg L^{-1} SMX); E - sample at t_1 (50 mg L^{-1} SMX); F - sample at t_2 (<5 mg L^{-1} SMX); G - sample at t_3 (no SMX detected); b) A - Freshwater (matrix) without SMX and without irradiation; B - control without irradiation (50 mg L^{-1} SMX); C - control covered with aluminum at t_3 of irradiation (50 mg L^{-1} SMX); D - control covered with aluminum at t_3 of irradiation (100 mg L^{-1} SMX); E - sample at t_1 (50 mg L^{-1} SMX); F - sample at t_2 (<5 mg L^{-1} SMX); G - sample at t_3 (no SMX detected); c) A – Estuarine water (matrix) without SMX and without irradiation; B - control without irradiation (50 mg L^{-1} SMX); C - control covered with aluminum at t_3 of irradiation (50 mg L^{-1} SMX); D - control covered with aluminum at t_3 of irradiation (100 mg L^{-1} SMX); E - sample at t_1 (50 mg L^{-1} SMX); F - sample at t_2 (<5 mg L^{-1} SMX); G - sample at t_3 (no SMX detected); d) A - STPF (matrix) without SMX and without irradiation; B - control without irradiation (50 mg L^{-1} SMX); C - control covered with aluminum at t_3 of irradiation (50 mg L^{-1} SMX); D - control covered with aluminum at t_3 of irradiation (100 mg L^{-1} SMX); E - sample at t_1 (50 mg L^{-1} SMX); F - sample at t_2 (<5 mg L^{-1} SMX); G - sample at t_3 (no SMX detected). Statistical hypothesis test: *ρ value = 0.05; **ρ value = 0.01; ***ρ value = 0.001.

Fig. 5: Mineralization of SMX along with direct photodegradation expressed as percentage of total organic carbon reduction (C/C_0). For comparison purposes, results are shown together with the corresponding percentage of *Vibrio fischeri* viable cells and percentage of SMX concentration decrease (C/C_0) in A - Ultrapure water (matrix) without SMX and without irradiation; B - control without irradiation (50 mg L^{-1} SMX); C - control covered with aluminum at t_3 of irradiation (50 mg L^{-1} SMX); D - control covered with aluminum at t_3 of irradiation (100 mg L^{-1} SMX); E - sample at t_1 (50 mg L^{-1} SMX); F - sample at t_2 (<5 mg L^{-1} SMX); G - sample at t_3 (no SMX detected).

Table 1: Parameters for the SMX photodegradation under continuous flow mode (this work) and under batch mode (Oliveira et al., 2019) (k (h^{-1}), $t_{1/2}$ (h)) and respective standard errors, obtained in ultrapure water and in environmental water matrices.

	This work		**Oliveira et al. (2019)**	
Sample	***k*** **(h^{-1})**	***$t_{1/2}$*** **(h)**	***k*** **(h^{-1})**	***$t_{1/2}$*** **(h)**
Ultrapure water	2.1 ± 0.2	0.32 ± 0.03	0.81 ± 0.04	0.86 ± 0.04
Estuarine water	0.49 ± 0.04	1.4 ± 0.1	0.13 ± 0.01	5.3 ± 0.5
Freshwater	0.69 ± 0.04	1.01 ± 0.06	0.117 ± 0.007	5.9 ± 0.4
STPF	0.47 ± 0.03	1.5 ± 0.1	0.092 ± 0.003	7.54 ± 0.04

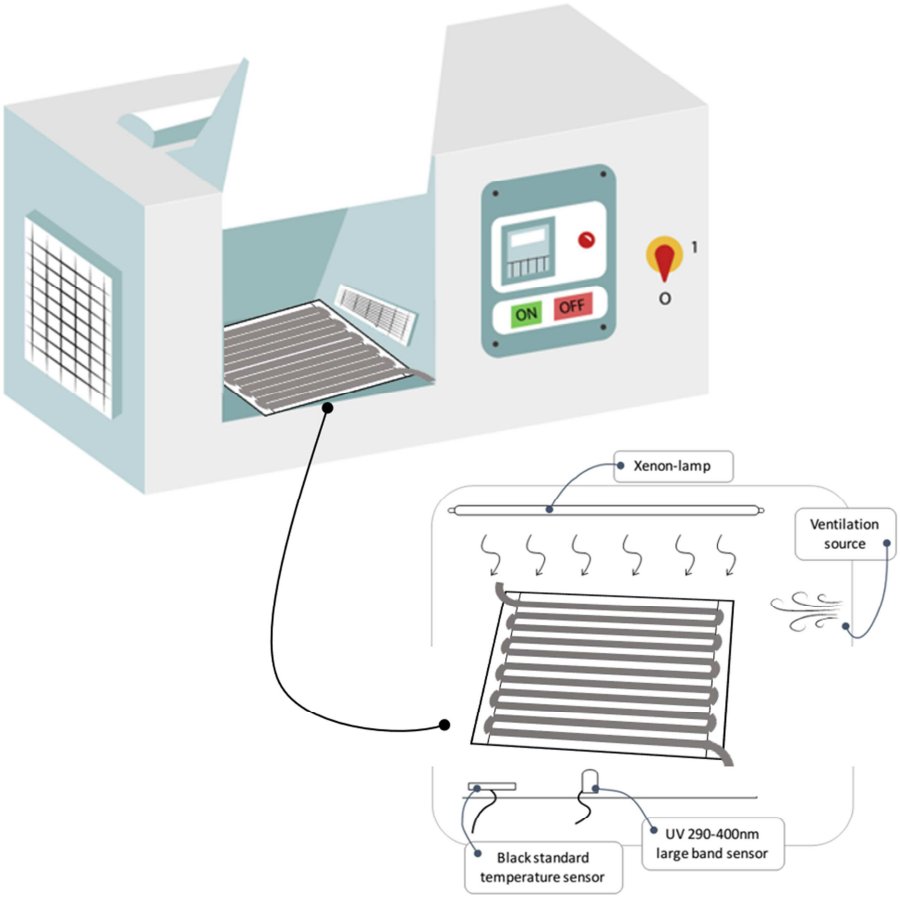
ON
OFF
1
0
Xenon-lamp
Ventilation source
Black standard temperature sensor
UV 290-400nm large band sensor

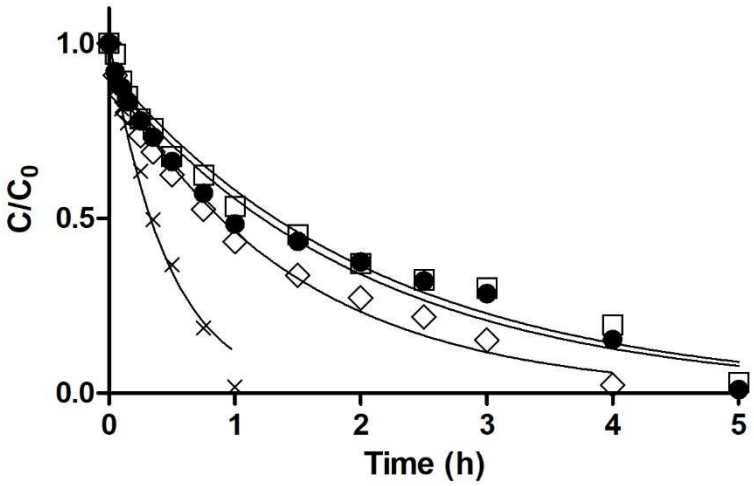

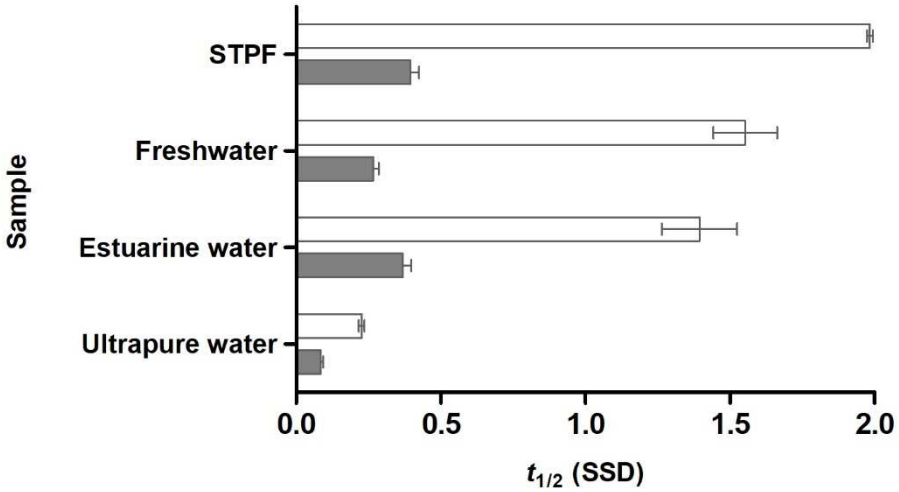

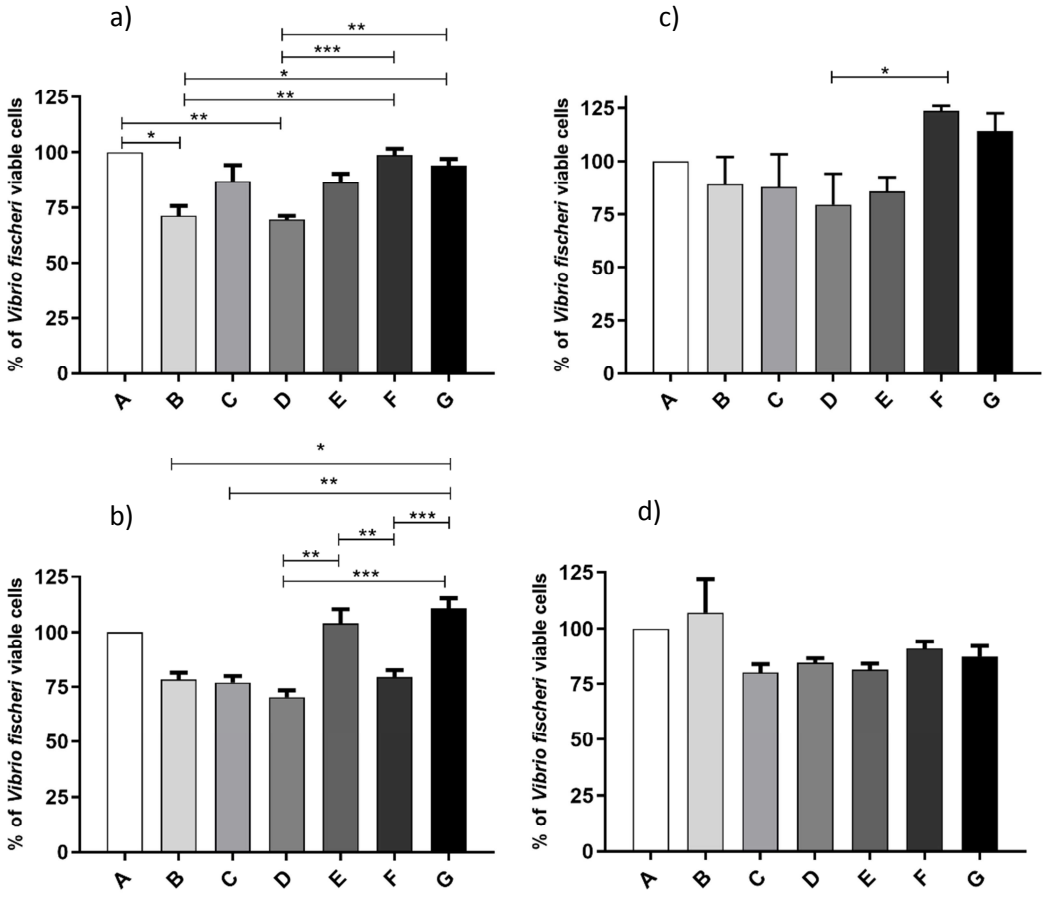
a)
c)
b)
d)
% of Vibrio fischeri viable cells
0
25
50
75
100
125
A
B
C
D
E
F
G
*
**
***

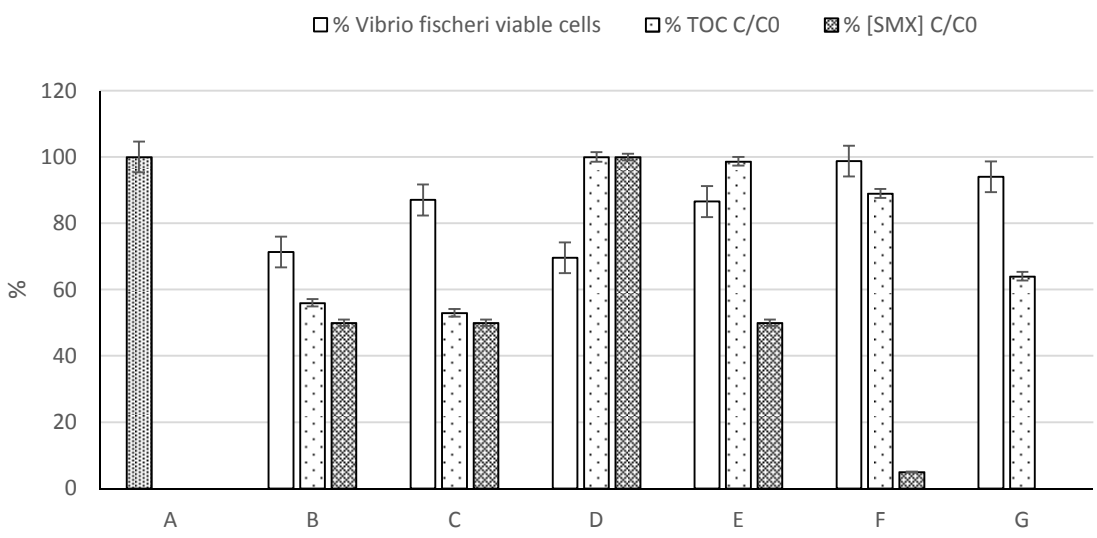

Highlights

- Photodegradation may appear as an alternative process for the removal of antibiotics
- Evaluation of continuous flow mode is essential as well as the antibacterial activity
- SMX photodegradation under continuous flow was much faster than in batch mode
- Photodegradation rate was higher in environmental waters than in ultrapure water
- Bacterial activity increased after SMX photodegradation